Article

Electronically Excited States of Closed-Shell, Cyano-Functionalized Polycyclic Aromatic Hydrocarbon Anions

Taylor J. Santaloci and Ryan C. Fortenberry *

Department of Chemistry & Biochemistry, University of Mississippi, University, MS 38677-1848, USA;
tsantalo@go.olemiss.edu
*   Correspondence: r410@olemiss.edu

Abstract: Few anions exhibit electronically excited states, and, if they do, the one or two possible excitations typically transpire beyond the visible spectrum into the near-infrared. These few, red-shifted electronic absorption features make anions tantalizing candidates as carriers of the diffuse interstellar bands (DIBs), a series of mostly unknown, astronomically ubiquitous absorption features documented for over a century. The recent interstellar detection of benzonitrile implies that cyano-functionalized polycyclic aromatic hydrocarbon (PAH) anions may be present in space. The presently reported quantum chemical work explores the electronic properties of deprotonated benzene, naphthalene, and anthracene anions functionalized with a single cyano group. Both the absorption and emission properties of the electronically excited states are explored. The findings show that the larger anions absorption and emission energies possess both valence and dipole bound excitations in the 450–900 nm range with oscillator strengths for both types of $>1 \times 10^{-4}$. The valence and dipole bound excited state transitions will produce slightly altered substructure from one another making them appear to originate with different molecules. The known interstellar presence of related molecules, the two differing natures of the excited states for each, and the wavelength range of peaks for these cyano-functionalized PAH anions are coincident with DIB properties. Finally, the methods utilized appear to be able to predict the presence of dipole-bound excited states to within a 1.0 meV window relative to the electron binding energy.

Keywords: dipole bound states; astrochemistry; anions; polycyclic aromatic hydrocarbons; electronically excited states; diffuse interstellar bands

1. Introduction

Excited states of anions are few and far between, but they are applicable in many areas of chemistry and materials science ranging from solar energy harvesting to astrochemical observation [1–5]. The reactivity and transience of anions creates difficulty for laboratory study but makes them excellent candidates for quantum chemical analysis. Fermi and Teller first probed the properties of anions via quantum mechanics finding that the binding energy of excess electrons is dependent upon the dipole moment of the corresponding neutral [6]. The dipole moment should be greater than 1.625 D in order to possess a first dipole bound state, but, practically, it should be at least greater than 2.00 D as studies have since indicated [7–15]. Additionally, dipole moments above this value will have a higher likelihood of exhibiting dipole bound states implying a proportional relationship between the dipole moment and the electron binding energy (eBE) [7,8,16–18].

CH_2CN^- and CH_2CHO^- were the first experimental examples of organic anions documented with dipole bound excited states [9,19–21]. Excitations into these states involve promotion of a valence electron into a highly diffuse, Rydberg-like orbital and transpire in the visible and near-infrared region of the electromagnetic spectrum [22]. These properties led Sarre to examine the A ^{1}B$_1$ ← X̃ ^{1}A′ dipole bound excitation of CH_2CN^- at 8037.78 Å for

its coincidence with an astronomical absorption peak at 8037.8 ± 15 Å [23,24]. The similarity of the two excitation energies led him to the currently unrefuted hypothesis that dipole bound anions are possible carriers for some of the diffuse interstellar bands (DIBs).

The DIB absorption lines have been observed towards innumerable interstellar sight-lines with surprising consistency in the signal, have been recorded for more than century, and occur in the visible and near-infrared regions [23,25,26]. In fact, the highest concentration of DIB features are in wavelengths longer than green. The rotational substructure of the peaks has led to the conclusion that these features are molecular in origin, but few of the peaks appear to be related. Unfortunately, only four of the hundreds of peaks have been currently attributed to specific molecular carriers [27,28]. Electronic transitions of C_{60}^{+}, conclusively observed in 2015, are linked closely to four of the DIBs [27] that reside in the near-infrared range. The rest of the DIBs remain unresolved.

Anions typically have lower energy excited states than cations and neutrals due to the weak association of the additional electron. This causes the eBE to be lower than the ionization potential of an uncharged molecule [22]. Incident energy above the eBE in the anion would most likely remove the excess electron instead of exciting it for absorption. Similarly, anions will only have one or two excited states, if any at all, implying that any spectrum containing them will require numerous different species to fill the census of peaks [29,30]. Consequently, anion wavelengths and absorption characteristics are longer and solitary making them tantalizing candidates for being carriers of the DIBs as has been proposed for CH_2CN^- [23,24].

Anions appear in varied astrophysical environments including the interstellar medium (ISM), planetary nebulae, and molecular clouds. Even so, they have only been on the roster of astronomically-known molecules for less than two decades even though they were proposed well before the turn of the last century [31–45]. Polycyclic aromatic hydrocarbons (PAHs) are also predicted to be distributed throughout space, as well, but the first detection of one of these is even more recent. While buckyballs (C_{60}) have been known for the past decade [46], benzontrile, simply a cyano-functionalized benzene, was first observed towards TMC-1 via rotational spectroscopy less than two years ago [47], confirming the long-held belief that PAHs are likely omnipresent in the ISM. Additionally, Saturn's moon Titan has produced evidence, initially during the *Voyager* mission, that its atmosphere contains a variety of hydrocarbons, which are building blocks for PAHs [48–56], in addition to a wealth of nitrogen chemistry. More than 25 years later, the *Cassini* mission found heavy anions in Titan's atmosphere ranging from 10–200 amu. The smaller masses are likely atomic anions and small molecules such as CN^-, but the larger species could be nitrogen-containing PAH anions [55,57–60]. PAH anions may be additional candidates for application to the carriers of various astronomical spectral features including the DIBs. In fact, excited states of the cation forms have been shown to take place in energetic regions close to the DIBs [61].

To explore the nature of dipole bound anions, proper quantum chemical treatment of such charged molecules requires a sufficient choice of basis set. Adding additional diffuse functions to standard correlation consistent basis sets can effectively describe dipole bound anion states, but this is a computationally expensive approach at the t-aug-cc-pVDZ (tapVDZ) level and beyond [17,62]. Adding just four hydrogen such as s-type diffuse functions (+4s) on a dummy atom either at the center of charge (COC) or center of mass (COM) to aug-cc-pVDZ (apVDZ) can make the computation less expensive. Dipole bound excited state energies for closed-shell, deprotonated anions of quinoline are practically identical for tapVDZ and aug-cc-pVDZ+4s (apVDZ+4s), but the latter reduces the basis set by 48%, thus reducing the computational cost and time [63]. In addition, adding more, dummy-atom-centered diffuse functions further increases the accuracy of describing dipole bound excited states. The aug-cc-pVDZ+6s6p2d (apVDZ+6s6p2d) basis set with these additional, hydrogen-like functions provides the limit at which more basis functions stop changing the effective excitation energy for rovibronic analysis of c-C_3H^- [64]. Consequently, dipole bound excited states with just the +4s functions added

on to the apVDZ basis set are not likely sufficient for quantitatively computing dipole bound excited state energies, but the +6s6p2d functions give indication of being such. Differently, valence excited states, by their very nature, do not require such extensively diffuse orbitals. Additional diffuse functions are not subsequently needed to study valence excited states of singly deprotonated PAH anions, but they are often included since the valence and dipole excited states are computed during the same run [65].

The present work builds upon previous studies [63,65,66] to provide further analysis for computing the electronically excited states of singly deprotonated PAH anions functionalized with a single cyano group. The cyano-functionalized PAH stabilities, eBEs, and electronically excited states are explored herein in a manner similar to previous studies with smaller molecules [62] but where the +6s6p2d orbitals may be required [67]. The cyano group is chosen for its behavior as an exceptionally strong electron withdrawing group which should increase the dipole moment even more than that predicted is with PANHs [63] and for its obvious relevance to the discovery of benzonitrile [47]. Extending the rings increases the likelihood of more excited states, as previously shown with related PANH and PAH anions [63,65,66]. Thus, the additional cyano group should affect photophysical properties more so than simple inclusion of nitrogen heteroatoms in the PAH structure and open the door for new photophysics of anions in various astrophysical environments or for other applications of anions.

2. Computational Details

Benzene, naphthalene, and anthracene are singly deprotonated and functionalized with a cyano group to create closed-shell anions and corresponding open-shell neutrals. There are multiple positions for the cyano group, and each is explored in this work. The methods utilized here are similar to approaches done previously for other closed-shell anions [63,65–67]. Geometry optimizations of the neutral radical and closed-shell anions utilize B3LYP/apVDZ [68] within Gaussian16 [69]. These optimizations provide the relative energies, dipole moments of the neutral radicals, and geometries for both the closed-shell anions and the corresponding neutral radicals. Additionally, the relative energies of the neutral radicals and anions are compared between B3LYP, MP2 [70], and ωB97XD [71] for benzonitrile in order to assess the performance of the various methods. Previous work shows B3LYP provides sufficient optimized structures for larger molecular systems especially for subsequent excited state analysis [63,65,66,72].

Vertical excited states of the anion and radical geometries utilize both CFOUR [73] and MOLPRO [74] with equation of motion coupled cluster theory at the singles and doubles level (EOM-CCSD) [75–77]. The basis set is augmented with six s-type, six p-type, and two d-type basis functions as past studies have shown is necessary [64,65,78–80]. Furthermore, two additional *s*-type diffuse functions are added onto the apVDZ+6s6p2d basis set (the apVDZ+8s6p2d basis set) for the benzene and naphthalene class in order to determine if a higher number of diffuse functions are needed to properly characterize the anion. In either case, the diffuse functions can be localized as ghost atoms at either the center of charge (COC) or center of mass (COM). Similar to the cyanoamide anions [67], the dummy atom placement for the COC is determined at the positive end of the radical dipole moment whether the actual geometry utilized is that for the optimized neutral radical or anion geometry.

The COM excitations have the dummy atom's additional diffuse orbitals placed at the COM, which is also the origin coordinate. Past work on cyanoamide anions shows that a lower energy wavefunction is produced by placing diffuse orbitals on the COC and is less likely not to destabilize occupied molecular orbitals as seen with the $NCNC_2H^-$ anion [67]. As with previous work [67], the vertically excited states computed from the optimized anion geometry are interpreted here to be absorption behavior since the closed-shell anion is being excited. Excitations from the radical geometry can be viewed as emission (with opposite sign of the energy) from the dipole bound excited state since the radical and

dipole bound geometries should be synonymous. The DIBs represent absorption leading most of the present discussion toward that end, but emission spectra are also reported.

The eBEs are computed to determine the maximum amount of energy that can produce an excited state before the electron dissociates. They are computed using EOM-CCSD with the ionization potential formalism (EOMIP) [81] with the apVDZ basis set in the CFOUR program [73,77,81,82]. Additional diffuse functions are not needed since the electrons in the radical are valence by construction. As a benchmark, the experimental eBE value for CH_2CN^- is 1.543 eV, and the computed value using EOMIP-CCSD/apVDZ is 1.524 eV, a difference of only 0.02 eV [9,17,19,24,79].

3. Results

The point groups for these closed-shell, cyano-functionalized PAH anions are either C_s or C_{2v}. Consequently, the excited states are either $^1A'/^1A_1$ or $^1A''/^1B_1$. The highest occupied molecular orbital (HOMO) is the lone pair on the carbon from where the hydrogen is removed. The transition into the $^1A'/^1A_1$ state involves an electron exciting out of the HOMO into a large, diffuse dipole bound orbital. The $^1A''/B_1$ state is created from the HOMO exciting into a π^* valence, particle-in-a-box (PIB) lowest unoccupied molecular orbital (LUMO). The transition into the $^1A''/^1B_1$ state is independent of the radical's dipole moment, but that into the $^1A'/^1A_1$ is not. In order for the transition into the $^1A'/^1A_1$ state to occur, the corresponding neutral radical needs to possess a large enough dipole moment. Again, 2.00 D is generally accepted, and the present study bears this out with all anions displaying dipole bound excited states and all with dipole moments of greater than 2.00 D. Finally, if a $^1A'/^1A_1$ or $^1A''/^1B_1$ state is below the eBE by more than 1.0 meV, our methodology will classify it as a physically-likely excited state for absorption.

3.1. Benzenonitrile

3.1.1. Relative Energies and Dipole Moments

The three different isomers of the anions/radicals for deprotonated benzonitrile are labeled in Figure 1. The numbers show the position where the hydrogen is removed. For example, radical/anion 4 has the hydrogen removed *para* to the cyanofunctional group. When the singly-occupied HOMO is next to the cyano group, the radical is the least stable. Consequently, radical 4 is the lowest energy isomer in Table 1 and is *para* to the functional group. Radical 2 is the highest energy isomer and is greater in energy by 0.0531 eV. Radicals 3 and 4 do not have a significant difference in energy. ωB97XD agrees with B3LYP qualitatively with the ωB97XD results typically 0.01–0.02 eV higher in energy. Slightly differently, MP2 shows that the least stable is radical 2, but radical 3 is shown as the most stable. Isomers 3 and 4 for either the radical or the anion are nearly degenerate, and this trend is maintained between MP2, ωB97XD, and B3LYP. Conversely for the anions, the stability increases the closer the anion lone pair is to the electron withdrawing group, the opposite trend from the radicals. Anion 4 is the least stable, while anion 2 is the most stable, as shown in Table 1. The same trend appears for the MP2 and ωB97XD computations in Table 1, further implying that the B3LYP data for this and the other species are likely reliable.
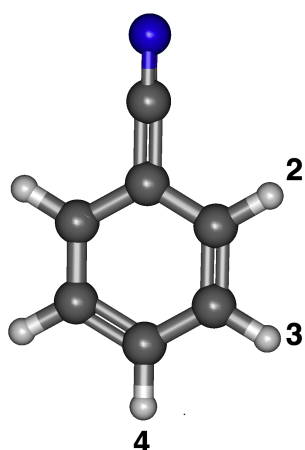
Figure 1. The optimized structure of benzonitrile with numbered positions of deprotonation.

Table 1. Relative Energies and Dipole of Benzonitrile.

B3LYP	Radical Rel.E (eV)	Anion Rel.E (eV)	Radical Dipole (D)
2	0.0531	0.0000	5.18
3	0.0065	0.0771	4.28
4	0.0000	0.0576	3.82
MP2	**Radical Rel.E (eV)**	**Anion Rel.E (eV)**	
2	1.1507	0.0000	
3	0.0000	0.0449	
4	0.0284	0.0863	
ωB97XD	**Radical Rel.E (eV)**	**Anion Rel.E (eV)**	
2	0.0634	0.0000	
3	0.0137	0.0986	
4	0.0000	0.0764	

As long as the neutral radical dipole moment is above 2.00 D, the anion should theoretically withstand dipole bound excitation. All of the dipole moments for the neutral radical isomers of benzonitrile are greater than 2.00 D. The highest dipole moment is radical 2 at 5.18 D, and the lowest is radical 4 at 3.82 D, as shown in Table 1. These dipolar data reveal that all three isomers of benzonitrile are likely to stabilize an electron attached in a dipole bound orbital.

3.1.2. Vertical Excitation Energies

Table 2 shows the excited states for benzonitrile's deprotonated anion isomers. The dipole bound transition is the $2\,^1A_1/2\,A^{'}$ state. These transition energies for anions 2–4 into the $2\,^1A_1/2\,A^{'}$ state are, respectively, underneath the eBE by 21.6, 12.6, and 3.4 meV. The amount below the eBE, while seemingly minuscule, is actually a clear characteristic of a dipole bound excited state. The right side of Figure 2 shows the diffuse s-type, Rydberg/dipole bound, accepting, virtual orbital for the $2\,^1A'$ dipole bound state of anion 2. The left side of Figure 2 depicts the donating, lone pair HOMO. The orbitals in anions 3 and 4 are similar even with the higher symmetry of anion 4. However, the $2\,^1A_1$ state of anion 4 is less than 10.0 meV underneath the eBE, and, therefore, additional diffuse functions have been added to probe the dipole bound nature of this anion. Inclusion of a larger apVDZ+8s6s2d basis shifts this excitation energy for this state by only 1.37 meV and the rest of the benzonitrile excitation energies by only 0.26 meV on average implying that our basis set is complete and that even this 3.4 meV difference from the eBE will still produce a dipole bound excited state.

Table 2. Vertical excitation energies (eV), eBEs, at the center of charge (COC) and center of mass (COM) for benzonitrile derivative anions.

| Abs [a] COC	$2\,^1A_1/2\,^1A'$	$3\,^1A_1/3\,^1A'$	$1\,^1B_1/1\,^1A''$	$2\,^1B_1/2\,^1A''$	$1\,^1B_2/4\,^1A'$	$2\,^1B_2/5\,^1A'$	$1\,^1A_2/3\,^1A''$	$2\,^1A_2/4\,^1A''$	eBE (eV)
2	2.3003	2.3233	2.3302	2.3575					2.3219
3	2.1393	2.1546	2.1616	2.1898					2.1519
4	2.2196	2.2305	2.2374	2.2659	2.2371	2.2628	4.1895	3.1359	2.2230
COM									
2	1.4254	1.4478	1.4548	1.4821					1.4454
3	1.3059	1.3222	1.3293	1.3584					1.3156
4	1.3568	1.3637	1.3710	1.4040	1.3707	1.4017	4.2450	1.4017	1.3607
Emission COC	$2\,^1A_1/2\,^1A'$	$3\,^1A_1/3\,^1A'$	$1\,^1B_1/1\,^1A''$	$2\,^1B_1/2\,^1A''$	$1\,^1B_2$	$2\,^1B_2$	$1\,^1A_2$	$2\,^1A_2$	eBE (eV)
2	1.4254	1.4478	1.4548	1.4821					1.4454
3	1.3059	1.3222	1.3293	1.3584					1.3156
4	1.3568	1.3637	1.3710	1.4040	1.3707	1.4017	4.2450	2.1496	1.3607

[a] Abs is absorption.
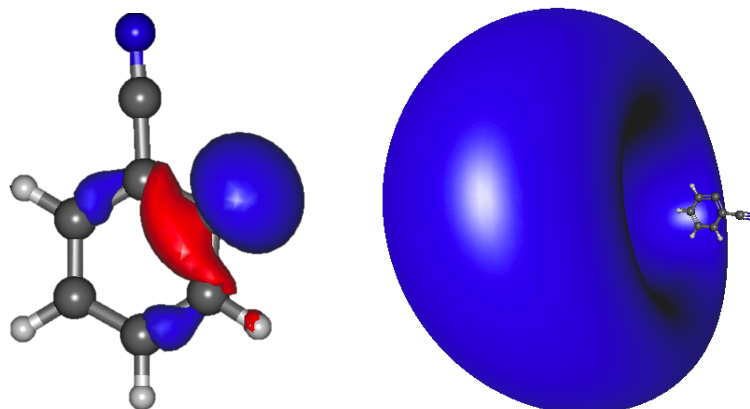
Figure 2. Benzonitrile anion 2 a′ HOMO (**left**) and the a′ LUMO (**right**) dipole bound orbital.

The placement of the ghost atom hosting the diffuse orbitals matters to a small, but potentially meaningful extent, as shown in Table 1. For instance, in anion 4, the difference between the COC and COM for the transition energy of the $2\,^1A_1$ state shifts the excitation energy enough to fall below the eBE. The excited state energy should be variational even within coupled cluster theory, implying that the COM orbitals produce the more physically-meaningful excitation energy. For most of the states computed, however, the COC-based excited state energies are lower in energy, and this position for the diffuse orbitals is maintained from here on.

While the radical and anion geometries have no discernible visible differences between them (as shown for the HOMOs in Figure 3), they vary enough to destabilize the orbitals and increase the relative energy of the anion wavefunction at this geometry which is not optimized for the lowest energy state wavefunction of the closed-shell anion. The HOMO orbital energies remain negative but close the HOMO–LUMO gap. This implies that "absorption" from the radical geometry will be lower in energy, but the Franck–Condon principal utilized in vertical excitations computed here implies that any process of absorption must originate with the ground electronic state structure present before the incident electron interacts with the molecule. This is the closed-shell anion structure, and the absorption of energy from the anion geometry will be higher in energy. While the molecule should relax to the radical geometry upon excitation, the electron dynamics will be initially governed by the wavefunction present in the closed-shell anion. Hence, absorption related to the DIBs or any other phenomena will depend upon the anion geometry.
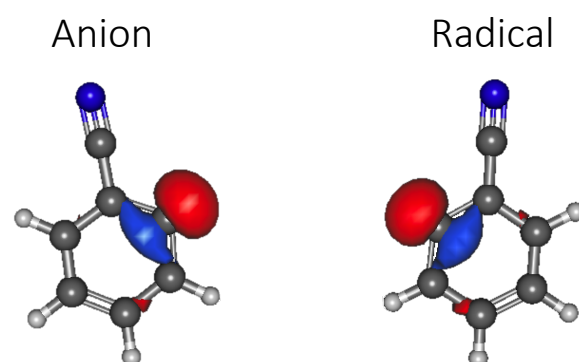

Figure 3. Benzonitrile anion geometry 2's *a′* HOMO (**left**) and the radical geometry 2's *a′* HOMO (**right**).

The vertical release of energy (emission) from returning down to the valence, closed-shell anion geometry from the radical geometry in a dipole-bound state will correspond to the energy difference between states at the radical geometry. The energy difference between these $^1A'$ states per choice of reference geometry has a mean value of 0.8570 eV,

as determined from values in Table 2. Hence, the energy difference between the valence ground and dipole bound excited state potential energy surfaces is much less at the radical geometry than the anion geometry. Again, however, any absorption phenomena such as the DIBs will require the reference geometry to be that of the closed-shell anion giving a much higher excitation energy.

The oscillator strengths (intensities) for the various deprotonated isomers are given in the Supplementary Materials. They follow the same trend as the previously explored PAH and PANH anions [63,65,66]. The dipole bound excited state oscillator strengths are on the order of 1×10^{-3}. While these are not notably large intensities, they are large enough to contribute to possible astronomical spectra, especially if these types of molecules are as common as believed for related species [47].

3.2. Cyanonaphthalene
Relative Energies and Dipole Moments

In Figure 4, 1-cyanonaphthalene has the cyano group on the inner part of the two rings, and 2-cyanonaphthalene has it on the outer part. In addition, the eight different anion/radical isomers for both cyanonaphthalene structures are labeled in Figure 4. For 1-cyanonaphtalene, anion 2 is the least stable and anion 7 is the most, as shown in Table 3. Radicals show the opposite trend. Radical 7 is the most stable and the least stable is radical 2, as also shown in Table 3. Radical 8 has the greatest dipole moment of 5.46 D and the smallest is radical 5 at 3.88 D. This leads to the possibility that all eight anions can have at least a dipole bound excited state.
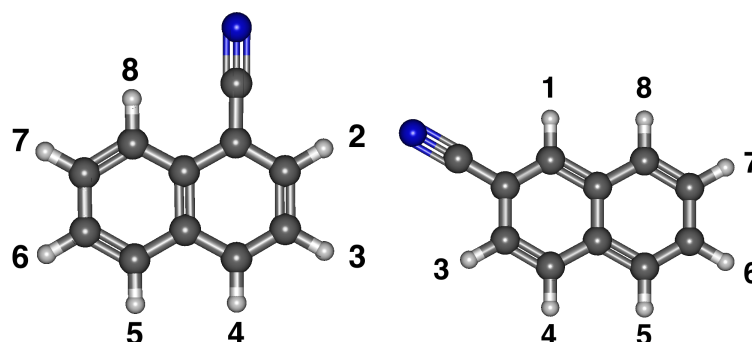

Figure 4. The optimized structure of both derivatives of cyanonaphthalene with numbered positions for deprotonation.

Table 3. Relative Energies and Dipole of Cyanonaphthalenes.

1-Cyano	Radical Rel.E (eV)	Anion Rel.E (eV)	Radical Dipole (D)
2	0.0500	0.0000	5.36
3	0.0176	0.0923	4.40
4	0.0027	0.0140	4.00
5	0.0072	0.1584	3.88
6	0.0003	0.2799	4.15
7	0.0000	0.3102	5.15
8	0.0306	0.2827	5.46
2-Cyano	**Radical Rel.E (eV)**	**Anion Rel.E (eV)**	**Radical Dipole (D)**
1	0.0634	0.0000	5.84
3	0.0701	0.1391	5.82
4	0.0178	0.1400	5.14
5	0.0123	0.2201	4.75
6	0.0000	0.2742	4.30
7	0.0066	0.3002	4.76
8	0.0149	0.2024	5.48

For the 2-cyanonaphthalene anion isomers, the most stable is anion 1 and least is anion 7, as given in Table 3. Alternatively, radical 6 is the most stable and radical 3 is the least, as provided in Table 3. Although the trend is not exactly the same as 1-cyanonaphthalene, the basic idea is still the same. Radicals are stabilized by being farther away from the hydrogen removal site, while, conversely, anions are stabilized by being closer to it. The largest dipole moment for the 2-cyanonaphthalene set is radical 1 at 5.84 D and the smallest is 4.30 D for radical 6. This shows that all the anions for 2-cyanonaphthalene are capable of possessing a dipole bound state.

When examining the lowest energy radical/anion isomer of both derivatives of cyanonapthalene, 2-cyanonaphthalene is lower in energy than 1-cyanonaphthalene for both the radical and anion isomers. Specifically, the lowest energy isomer of 1-cyanonaphthalene is radical 7, which is 9.8 meV above 2-cyanonaphthalene radical 6. Additionally, 1-cyanonaphthalene anion 2 is 9.5 meV above the 2-cyanonaphthalene anion 1 energy. The placement of the cyano group causes the box from the PIB analogy to become longer, which lowers the energy of the 2-cyanonaphthalene in general relative to the other isomer.

For both of the naphthalene isomers, the dipole bound state is the $2\,^1A'$ state, and the valence state is the $1\,^1A''$ state, as shown in Table 4. Similar to the benzonitrile derivatives, all of the dipole bound state energies for both cyanonaphthalenes isomers are underneath the eBE.

Table 4. Anion derivative absorption energies and eBE, neutral radical dipole moments, and neutral radical and anion relative energies for the cyanonaphthalene deprotonated derivatives.

1-Cyanonaph.	Excited States		eBE (eV)
	$2\,^1A'$	$1\,^1A''$	
2	2.5287	2.5544	2.5463
3	2.3528	2.3721	2.3635
4	2.4862	2.4797	2.4944
5	2.2953	2.3131	2.3017
6	2.1671	2.1880	2.1789
7	2.1402	2.1677	2.1595
8	2.1653	2.1897	2.1815
2-Cyanonaph.			
1	2.6229	2.6411	2.6332
3	2.4745	2.3465	2.4848
4	2.3751	2.3906	2.3822
5	2.2890	2.3238	2.3142
6	2.2791	2.2851	2.2931
7	2.2174	2.1070	2.2438
8	2.3301	2.3708	2.3627

Unlike the benzonitrile isomers, 1-cyanonaphthalene has an isomer with what appears to be both a dipole bound and valence transition underneath the eBE. In anion 4, a valence transition falls underneath the eBE by 14.7 meV producing the $1\,^1A''$ state. This behavior results from an increase in the size of the box for the PIB valence electronic structure in moving from the smaller benzonitrile to the larger naphthalene. All of the electronic properties of these anions fall in the wavelength range of 496–591 nm. 1-cyanonaphthalene deprotonated anion derivatives produce a total of eight anions with a dipole bound excited state and one with both a dipole bound and valence excited state.

The oscillator strengths for the singly-deprotonated 1-cyanonaphthalene anion isomers are, again, given in the Supplementary Materials. They show the same $\sim 1 \times 10^{-3}$ intensities in line with benzonitrile. The anion 2 valence excited state f value is even lower at 2×10^{-6}. This is, once more, in line with previous examination of related species [63,65,66]. Consequently, the dipole bound states are likely more important for any application to the largest DIBs. Any valence states would not be nearly as observable.

The lower half of Table 4 shows the electronically excited states for 2-cyanonaphthalene. Similar to 1-cyanonaphthalene, all of the dipole bound transitions are underneath the eBE. In addition, similar to 1-cyanonaphthalene, some dipole bound transition energies are barely underneath the eBE. An example is 1-cyanonapthalene anion 5. Its transition energy is 6.4 meV below the eBE. Another example is 2-cyanonapthalene anion 4, which is similar at 7.2 meV below the eBE. Similar to benzonitrile, the EOM-CCSD/apVDZ+8s6p2d 2 $^1A'$ transition energy computations show an increase in the cyanonaphthalene derivatives apVDZ+6s6p2d 2 $^1A'$ state energies by a mere 0.115 meV not enough to provide any real quantitative (much less qualitative) improvement in the description of the dipole bound excitation energy. This confirms that the apVDZ+6s6p2d basis set is near the diffuse limit of the basis set, once more showing that the computational approach employed here is producing computations with 1.0 meV precision.

Interestingly, more transitions appear below the eBE when the cyano group is on the outer part of the rings. This is because the box, for the PIB analogy, gets longer, which increases the probability of the excitations falling underneath the eBE due to the smaller energy separations between states. Similar to 1-cyanonapthalene, anions 3, 6, and 7 have valence transitions. Figure 5 shows both the valence and dipole bound orbitals of anion 7. The far left is the HOMO lone pair, the valence state is next to it, and the dipole bound state is on the opposite side. The valence and dipole bound states for anions 6 and 7 have similar topologies as in Figure 5. These excitations are in the wavelength range of 470–553 nm; 24 unknown DIB peaks fall within this range [83]. Furthermore, anion 6 is the most stable anion, making it the most likely to exist in astrophysical regions where DIBs may be observed, and has both a dipole bound and valence excitation. The 1 $^1A''$ and 2 $^1A'$ valence and dipole bound excited states, respectively, for anion 6 are 2.2851 and 2.1070 eV, corresponding to wavelengths of 543 and 544 nm. Similarly, there are unidentified DIBs peaks at 541.84 and 544.96 nm. Additionally, the oscillator strength for the valence state of anion 6 is actually on par with that for the dipole bound state in this instance both on the order of 10^{-3} implying a possible additional significance for the valence 2 $^1A'$ state in this instance. There can be no conclusion made that these are possible DIB carriers, but, in the least, a notable coincidence is present.
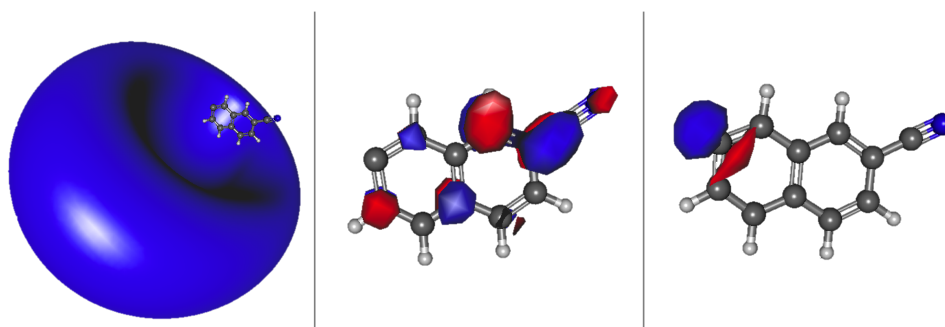

Figure 5. 2-cyanonaphthalene anion 7 a$'$ HOMO (**right**); a$''$ valence state π LUMO (**middle**); and a$'$ dipole bound state LUMO (**left**).

Similar to benzonitrile, the cyanonaphthalene absorption transition energies are larger than the emission. Interestingly, the average comparison between the $^1A'$ transition energies results in a larger average of 0.8869 eV, which is 0.0299 eV greater than the average benzonitrile absorption-emission energy differences. Separately, the 1-cyanonaphthalene mean absorption-emission energy difference average is 0.0056 eV greater than 2-cyanonaphthalene. A example of the absorption and emission difference calculation is demonstrated with the dipole bound energy transitions of 1-cyanonapthalene absorption and emission anion 2. The absorption energy of the 2 $^1A'$ state is 2.5287 eV, which is shown in Table 4, and the emission energy of the 2 $^1A'$ state is given in Table S2 and is 1.6249 eV. Hence, the absorption-emission energy difference would equal 0.9038 eV. As a result, the average in

the absorption-emission difference is negligible but indicates the more stable isomer has slightly less of a difference between the ground and excited state potential surfaces.

3.3. Cyanoanthracene
3.3.1. Relative Energies and Dipole Moments

Figure 6 shows three various positions for the cyano group on anthracene. 1-cyanoanthracene only has six different anion/radical isomers due to C_{2v} symmetry before deprotonation, but the others have ten distinct anion/radical isomers because of C_s symmetry. Similar to benzonitrile and cyanonaphthalene, the labels reference where the hydrogen is removed, and these positions are given in Figure 6.
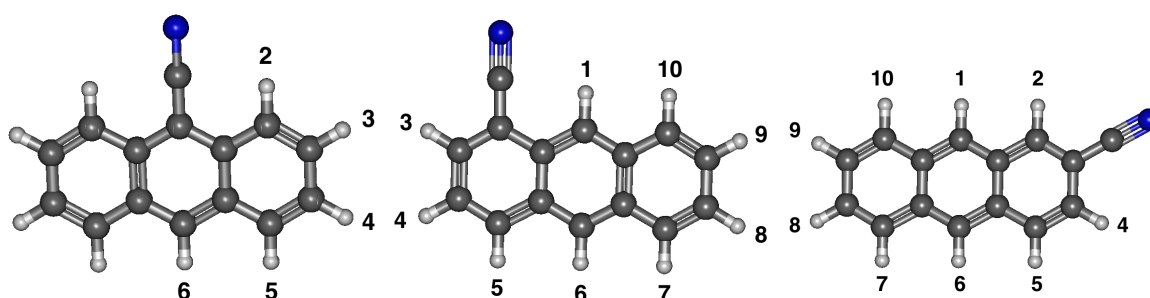
Figure 6. The optimized structure of cyanoanthracene derivatives with numbered positions for deprotonation.

Table 5 exhibits the relative energies and radical dipole moments for 1-cyanoanthracene. Unlike benzonitrile, the C_{2v} symmetry orientation of anion 6 (opposite from the cyano group) is the most stable. The least stable isomer of 1-cyanoanthracene is anion 3. Similar to benzonitrile and the cyanonaphthalenes, the least stable radical is closest to the cyano group in radical 2, while the most stable is radical 3. However, the size of the molecule causes less of an energy difference when removing the hydrogens. The result is that the other radicals are all within 0.0030 eV of each other and all of the radical dipole moments are within 1.50 D of each other. Radical 2 has the largest dipole moment of 5.48 D, but all of the other dipole moments are at least 4.00 D.

For 2-cyanoanthracene, Table 5 shows the energetic properties of both the anions and radicals. The middle of Figure 6 shows that 2-cyanoanthracene has the cyano group on the outer ring but in an interior position. Similar to the cyanonaphthalenes, the most stable anion isomer is the one closest to the cyano group, and the least stable is the farthest away. The opposite trend holds true for the radicals once more. Table 5 specifically shows that anion 3 is the most stable and anion 9 is the least. The most stable radical isomer is radical 8 and the least is radical 3. However, the energetic isomerization distinction between radicals 8 and 9 is only 0.0020 eV. All of the 2-cyanoanthracene radical isomer dipole moments are above 2.00 D. The greatest is radical 1 at 5.58 D, and the smallest is radical 7 at 4.01 D. As with benzonitrile, cyanonaphthalene, and the other isomer of cyanoanthracene, the neutral radical dipole moments increase when the hydrogen removal is closer to the cyano group. In addition, similar to 1-cyanoanthracene, the relative energies of the radicals are all at most within 0.0500 eV, which results in the dipole moments of the radicals to only vary by 1.60 D, less than 30%.

3-cyanoanthracene anion/radical derivatives relative energies, dipole moments and electronically excited states are also given in Table 5. The most stable is anion 2 and the least stable is anion 9 with a 0.3840 eV difference. The radical relative energy between the most and least stable is 0.0777 eV between radicals 8 and 4. Furthermore, all of the dipole moments are greater than 2.00 D with the smallest dipole moment being 5.00 D. Compared to the other cyanoanthracenes, the cyano group on the outer part of the ring increases the dipole moments more than the other derivative because the highest dipole moment for this entire study is radical 2 with a 6.32 D dipole moment. Upon first inspection, all 24 cyanoanthracenes anions can withstand a dipole bound excitation.

Table 5. Relative energies and dipole of cyanoanthracenes.

1-Cyano	Radical Rel.E (eV)	Anion Rel.E (eV)	Radical Dipole (D)
2	0.0323	0.4171	5.48
3	0.0000	0.4273	5.21
4	0.0063	0.4072	4.43
5	0.0096	0.2672	3.95
6	0.0095	0.0000	3.97
2-Cyano	**Radical Rel.E (eV)**	**Anion Rel.E (eV)**	**Radical Dipole (D)**
1	0.0436	0.1499	5.58
3	0.0556	0.0000	5.45
4	0.0277	0.1064	4.78
5	0.0090	0.0156	4.06
6	0.0197	0.0145	4.14
7	0.0063	0.2698	4.01
8	0.0000	0.3651	4.24
9	0.0020	0.3781	5.10
10	0.0198	0.3545	5.64
3-Cyano	**Radical Rel.E (eV)**	**Anion Rel.E (eV)**	**Radical Dipole (D)**
1	0.0290	0.0431	6.15
2	0.0621	0.0000	6.32
4	0.0777	0.1766	6.61
5	0.0211	0.1662	5.65
6	0.0215	0.1059	5.50
7	0.0111	0.3038	5.31
8	0.0000	0.3653	4.59
9	0.0074	0.3840	5.00
10	0.0074	0.2930	6.01

When comparing the lowest energy radical/anion isomer to the three derivatives of cyanoanthracene, the lowest energy anion is 1-cyanoanthracene, and the highest energy is 3-cyanoanthracene with the opposite trend true in the radicals. The high symmetry cyano position stabilizes the anion more than juxtaposition to the functional group in the case of 1-cyanoanthracene, but the low symmetry position farthest away from the functional group stabilizes the radicals.

3.3.2. Vertical Excitation Energies

Table 6 also displays the electronically excited states of the deprotonated cyanoanthracene anions. Similar to benzonitrile, 1-cyanoanthracene anion 6 is C_{2v} symmetry with the $2\,^1A_1$ state being dipole bound and the $1\,^1B_1$ valence. Similar to benzonitrile, all of the other 1-cyanoanthracene isomers are C_s, which indicates that the $2\,^1A'$ state is dipole bound, and $1\,^1A''$ is valence. *All* of the anions have both dipole bound and valence states that are greater than 1.0 meV below the eBE. The dipole bound excited state of anion 5 at 12.5 meV below the eBE is the closest of the set. The proximity of the dipole bound transition energy to the eBE is, again, typical dipole bound behavior. All of the 1-cyanoanthracenes excitation wavelengths are greater than 619 nm and all have oscillator strengths greater than 1×10^{-4} even for the valence states.

For the other two cyanoanthracene sets, the dipole bound state is the $2\,^1A'$ and the valence is the $1\,^1A''$ in all eighteen isomers. For the 2-cyanoanthracene class, the transition energies for anion isomers 3, 4, 5, 8, 9, and 10 are all below the eBE. All of the 2-cyanoanthracene anions can exhibit dipole bound excited states. Similar to benzonitrile, cyanonaphtalene, and 1-cyanoanthracene the $2\,^1A'$ states are close in the energy to the eBE. However, all 9 anions have valence excited states. The valence state excitation energies range from 592 to 747 nm, once more in a range fitting for DIB transitions. Again, all of the oscillator strengths are stronger than the cyanonaphthalenes at $>1 \times 10^{-4}$.

Table 6 shows the excited state information for 3-cyanoanthracene. All of the dipole moments are large enough the stabilize a dipole bound state, and all of the 3-cyanoanthracene dipole bound transitions states are below the eBE. Anion 10 differs the most from the eBE and is 45.2 meV underneath the eBE. The closest dipole bound state to the eBE is anion 4 and is only 3.0 meV lower in energy. Since the apVDZ+6s6p2d approaches the basis set limit for diffuseness of the basis set in the two smaller ring classes, no further additional diffuse functions are needed to confirm that all of the 3-cyanoanthracene isomers have a dipole bound state.

Table 6. Anion derivatives vertical excitation energies and eBE, neutral radicals dipole moments, and neutral radicals and anions relative energies for cyanoanthracene deprotonated derivatives.

1-Cyanoanthra. Abs.	Excited States		eBE (eV)
	$2\,^1A'/2\,^1A_1$	$1\,^1A''/1\,^1B_1$	
2	2.2284	1.2574	2.3085
3	2.2884	1.6124	2.3406
4	2.3079	1.5382	2.3295
5	2.4781	1.7714	2.4851
6 [a]	2.8127	2.1633	2.8250
2-Cyanoanthra.			
1	2.4945	2.0192	2.5035
3	2.6852	2.0828	2.7056
4	2.4985	1.7281	2.5103
5	2.6489	2.0650	2.6601
6	2.6355	2.0953	2.6453
7	2.3211	1.8081	2.3344
8	2.2214	1.6596	2.2367
9	2.2096	1.6689	2.2329
10	2.2218	1.7390	2.2422
3-Cyanoanthra.			
1	2.7098	2.1810	2.7281
2	2.7996	2.2930	2.8030
4	2.6041	1.9315	2.6071
5	2.5120	1.9978	2.5202
6	2.6091	2.1119	2.6240
7	2.3689	1.8407	2.3862
8	2.3294	1.7633	2.3583
9	2.2789	1.6846	2.3202
10	2.3785	1.8582	2.4237

[a] 1-cyanoanthracene isomer 6 is C_{2v}.

All 10 of the 3-cyanoanthracene anion isomers possess valence excited states. These excited states are spread across the visible spectrum from 443 to 738 nm. One such example of a 3-cyanoanthracene isomer with both a valence and dipole bound state is anion 7, which is pictured in Figure 7. For anion 7, the valence state transition is 1.8412 eV. This excitation is from the HOMO lone pair (bottom left) electron exciting into the PIB LUMO (top left). The dipole bound transition is higher in energy than the valence state and excites into the loosely bound Rydberg s-type orbital shown to the right of both the HOMO and PIB LUMO in Figure 7. The cyanoanthracene valence and dipole bound states involves similar orbitals to those given in Figure 7.
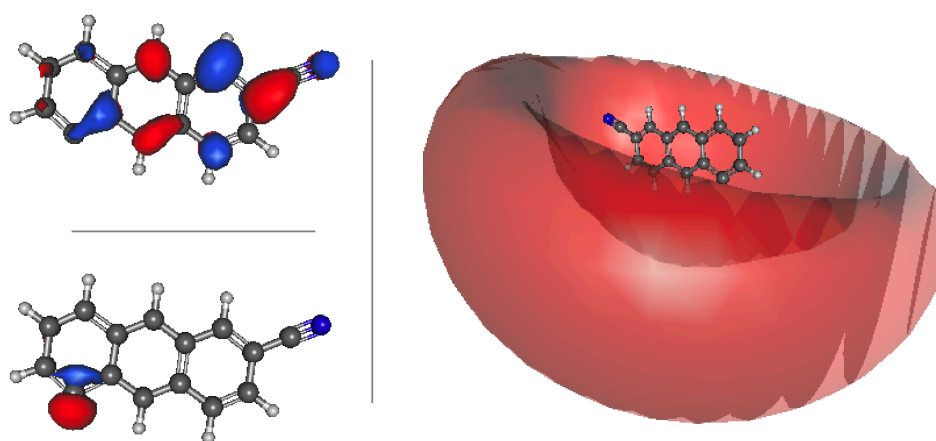
Figure 7. 3-cyanoanthracene anion 7 a′ HOMO (**bottom left**); a″ valence state π LUMO (**top left**); and a′ dipole bound state LUMO (**right**).

4. Conclusions

Once a deprotonated, closed-shell cyano-functionalized PAH anion contains three rings, it will exhibit at least one electronically excited valence state. This is similar to inclusion of nitrogen heteroatoms in related PANH anions where similar behavior was also observed for three rings [63,65]. However, pure PAH anions require at least four rings [66], unless, as this present work demonstrates, they are functionalized. The electron-withdrawing nature of the cyano group destabilizes the ring structure similarly to the N heteroatom. This produces closer gaps between the HOMO and LUMO allowing for valence excited states. Such behavior is most notable in the 1-cyanonaphthalene anion 4 isomer which is producing both dipole bound *and* valence excited states. The oscillator strengths for all of the dipole bound states are in the same $\sim 1 \times 10^{-3}$ *f* value range. Once the number of rings is three (and likely larger), the oscillator strengths of the valence excited states are of the same magnitude as their dipole bound relatives.

Every neutral radical explored in this paper has a dipole moment large enough to theoretically keep a electron bound in a dipole bound state of the corresponding closed-shell anion. Hence, all of the anions explored here should produce dipole bound excited states. This is presently shown and quantitatively given. The most meaningful data really are the relative differences between the dipole bound excited state energy and the eBE. Hence, the present work provides quantitative predictions for such relative energies. Furthermore, the excited states computed with the apVDZ+6s6p2d COC centered functions do not differ by more than 1.0 meV from the slightly larger apVDZ+8s6p2d basis even for dipole moments of corresponding neutral radicals of greater than 4.00 D. As a result, the accuracy for the EOM-CCSD/apVDZ+6s6p2d COC approach utilized here is in the range of approximately 1.0 meV relative to the eBE.

Deprotonation of PAHs will be most stable when the resulting lone pair is adjacent to the functional group unless symmetry distributions of the orbital space are present like in anion 6 of 1-cyanoanthracene. The radicals, however, will be most stable in the opposite trend where the singly-occupied orbital is farthest away from the functional group. The resonance of the lone pair in the anion with the π orbitals of the cyano group are constructive, but the single electron cannot fully create such a positive interaction. Even so, the relative energies between all isomers of a set are fairly small, implying that only extremely low-temperature regions, such as the ISM, will delineate deprotonated PAH isomers to any observable extent.

Furthermore, Sarre's dipole bound excited state anion hypothesis for the DIBs has been extended here to the titular molecules. The dipole bound and exhibited valence excited states of these various PAH anions all fall within the densest DIB field between 450 and 900 nm [83]. Additionally, the substructures of the valence and dipole bound excitation peaks will differ since the valence states will largely retain the structure of the anion, but the

dipole bound states will necessarily have the radical geometry. As a result, the valence and the dipole bound excited states of these closed-shell, deprotonated, functionalized PAH anions will appear to be caused by different molecules to some extent. However, further, experimental studies are needed to say conclusively whether these anions are carriers of the DIBs, but the present theoretical data support such a possible correlation.

References

1. Sidorkin, V.; Belogolova, E.F.; Doronina, E.P.; Liu, G.; Ciborowski, S.M.; Bowen, K.H. "Outlaw" Dipole Bound Anions of Intra-Molecular Complexes. *J. Am. Chem. Soc.* **2020**, *142*, 4. [CrossRef] [PubMed]
2. Castellani, M.E.; Anstöter, C.S.; Verlet, J.R.R. On the Stability of a Dipole-Bound State in the Presence of a Molecule. *PCCP Commun.* **2019**, *21*, 242826. [CrossRef]
3. Hendricks, J.; Lyapustina, S.; de Clercq, H.; Bowen, K. The Dipole Bound-to-Covalent Anion Transformation in Uracil. *T J. Chem. Phys.* **1998**, *108*, 8. [CrossRef]
4. Skurski, P. An Excess Electron Bound to Urea. I. Canonical and Zwitterionic Tautomers. *J. Chem. Phys.* **2001**, *115*, 8373. [CrossRef]
5. Boschloo, G.; Hagfeldt, A. Characteristics of the Iodide/Triiodide Redox Mediator in Dye-Sensitized Solar Cells. *Acc. Chem. Res.* **2009**, *42*, 1819–1826. [CrossRef] [PubMed]
6. Fermi, E.; Teller, E. The Capture of Negative Mesotrons in Matter. *Phys. Rev. J.* **1947**, *72*, 399–408. [CrossRef]
7. Turner, J.E.; Fox, K. Minimum Dipole Moment Required to Bind an Electron to a Finite Dipole. *Phys. Lett.* **1966**, *23*, 547–549. [CrossRef]
8. Mittleman, M.H.; Myerscough, V.P. Minimum Moment Required to Bind a Charged Particle to an Extended Dipole. *Phys. Lett.* **1966**, *23*, 545–546. [CrossRef]

9. Gutsev, G.L.; Adamowicz, L. The Valence and Dipole-Bound States of the Cyanomethide Ion, CH_2CN^-. *Chem. Phys. Lett.* **1995**, *246*, 245–250. [CrossRef]

10. Crawford, O.; Dalgarno, A. Bound States of an Electron in a Dipole Field. *Chem. Phys. Lett.* **1967**, *1*, 23. [CrossRef]

11. Jordan, K.D. Theoretical Study of the Binding of an Electron to a Molecular Dipole:LiCl⁻. *J. Chem. Phys.* **1976**, *64*. [CrossRef]

12. Turner, J. Minimum Dipole Moment Required to Bind an Electron-Molecular Theorist Rediscover Phenomenon Mentioned in Fermi-Teller Paper Twenty Years Earlier. *Am. J. Phys.* **1977**, *45*, 758–766. [CrossRef]

13. Crawford, O.H. Electron Affinities of Polar Molecular. *J. Chem. Phys.* **1977**, *66*, 4968–4970. [CrossRef]

14. Gutowski, M.; Skurski, P.; Boldrev, A.I.; Simons, J.; Jordan, K.D. Contribution of Electron Correlation to the Stability of Dipole-Bound Anionic States. *Phys. Rev. A* **1996**, *54*, 1906–1909. [CrossRef] [PubMed]

15. Jordan, K.D.; Wang, F. Theory of Dipole Bound Anions. *Annu. Rev. Phys. Chem.* **2003**, *54*, 367–396. [CrossRef]

16. Compton, R.; Carman, H.; Desfrancois, C.; Hendricks, J.; Lyapustina, S.A.; Bowen, K.H.; Abdoul-Carime, H.; Schermann, J.P. On the Binding of Electrons to Nitromethane: Dipole and Valence Bound Anions. *J. Chem. Phys.* **1996**, *105*, 3472–3478. [CrossRef]

17. Fortenberry, R.C.; Crawford, T.D. Theoretical Prediction of New Dipole-Bound Singlet States for Anions of Interstellar Interest. *J. Chem. Phys.* **2011**, *134*, 154304. [CrossRef] [PubMed]

18. Coulson, C.; Walmsley, M. The Minimum Dipole Moment Required to Bind an Electron to a Finite Electric Dipole. *Proc. Phys. Soc.* **1967**, *91*. [CrossRef]

19. Lykke, K.R.; Neumark, D.M.; Andersen, T.; Trapa, V.J.; Lineberger, W.C. Autodetachment Spectroscopy and Dynamics of CH_2CN^- and CD_2CN^-. *J. Chem. Phys.* **1987**, *87*, 6842–6853. [CrossRef]

20. Mullin, A.S.; Murray, K.K.; Schulz, C.P.; Lineberger, W.C. Autodetachment Dynamics of Acetaldhyde Enolate Anion, CH_2CHO^-. *J. Phys. Chem.* **1993**, *97*, 10281–10286. [CrossRef]

21. Mullin, A.S.; Murray, K.K.; Schulz, C.; Szaflarski, D.M.; Lineberger, W. Autodetachment Spectroscopy of Vibrationally Excited Acetaldehyde Enolate Anion, CH_2CHO^-. *Chem. Phys.* **1992**, *166*, 207–213. [CrossRef]

22. Fortenberry, R.C. Interstellar Anions: The Role of Quantum Chemistry. *J. Phys. Chem. A* **2015**, *119*, 9941–9953. [CrossRef] [PubMed]

23. Sarre, P. The Diffuse Interstellar Bands: A Dipole-Bound State Hypothesis. *Mon. Not. R. Astron. Soc.* **2000**, *313*, L14–L16. [CrossRef]

24. Cordiner, M.A.; Sarre, P.J. The CH_2CN^- Molecule: Carrier of the $\lambda 8037$ Diffuse Interstellar Band. *Astron. Astrophys.* **2007**, *472*, 537–545. [CrossRef]

25. Foing, B.; Ehrenfreund, P. Detection of Two Interstellar Absorption Bands Coincident with Spectral Features of C_{60}^+. *Nature* **1994**, *396*, 296–298. [CrossRef]

26. Maier, J.P. Interstellar Detection of C_{60}^+. *Nature* **1994**, *370*, 423–424. [CrossRef]

27. Campbell, E.; Holz, M.; Gerlich, D.; Maier, J. Laboratory Confirmation of C_{60}^+ as the Carrier of Two Diffuse Interstellar Bands. *Nature* **2015**, *523*, 322–323. [CrossRef]

28. Cordiner, M.A.; Linnartz, H.; Cox, N.L.J.; Cami, J.; Najarro, F.; Proffitt, C.R.; Lallement, R.; Ehrenfreund, P.; Foing, B.H.; Gull, T.R.; et al. Confirming Interstellar C_{60}^+ Using the Hubble Space Telescope. *Astrophys. J. Lett.* **2019**, *875*, L28. [CrossRef]

29. Czekner, J.; Cheung, L.F.; Johnson, E.L.; Fortenberry, R. A High Resolution Photoelectron Imaging and Theoretical Study of CP⁻ and C_2P^-. *J. Phys. Chem.* **2018**, *148*, 044301. [CrossRef]

30. Simons, J. Molecular Anions. *J. Phys. Chem.* **2008**, *112*, 6401–6511. [CrossRef]

31. Terzieva, R.; Herbst, E. Radiative Electron Attachment to Small Linear Carbon Cluster and its Significance for the Chemistry of Diffuse Interstellar Clouds. *Int. J. Mass Spectrom.* **2000**, *201*, 135–142. [CrossRef]

32. Millar, T.J.; Herbst, E.; Bettens, R.P.A. Large Molecules in the Envelope Surroundings IRC+10216. *Mon. Not. R. Astron. Soc.* **2000**, *316*, 195–200. [CrossRef]

33. McCarthy, M.C.; Gottlieb, C.A.; Gupta, H.; Thaddeus, P. Laboratory and Astronomical Identification of the Negative Molecular Ion C_6H^-. *Astrophys. J.* **2006**, *652*, L141–L144. [CrossRef]

34. Lepp, S.; Dalgarno, A. Polycyclic Aromatic Hydrocarbons in Interstellar Chemistry. *Astrophys. J.* **1988**, *324*, 533. [CrossRef]

35. Schild, R.; Chaffee, F.; Frogel, J.; Persson, S. The Nature of Infrared Excesses in Extreme Be Stars. *Astrophys. J.* **1974**, *190*, 73–83. [CrossRef]

36. Snow, T. A Search for H⁻ in the Shell Surrounding Chi Ophiuchi. *Astrophys. J.* **1975**, *198*, 361–367. [CrossRef]

37. Ross, T.; Baker, E.; Snow, T.; Destree, J.; Rachford, B. The Search for H⁻ in Astrophysical Environments. *Astrophys. J.* **2008**, *684*, 358–363. [CrossRef]

38. Tulej, M.; Kirkwoods, D.; Pachkov, M.; Maier, J. Gas-Phase Electronic Transitions of Carbon Chain Anions Coinciding with Diffuse Interstellar Bands. *Astrophys. J. Lett.* **1998**, *506*, L69–L73. [CrossRef]

39. Kawaguchi, K.; Kasai, Y.; Ichi Ishikawa, S.; Kaifu, N. A Spectral-Line Survey Observation of IRC+10216 between 28 and 50 GHz. *Publ. Astron. Soc. Jpn.* **1995**, *47*, 853–876.

40. Aoki, K. Candidates for U-Lines at 1377 and 1394 MHz in IRC+10216: Ab Intio Molecular Orbital Study. *Chem. Phys. Lett.* **2000**, *323*, 55–58. [CrossRef]

41. Brünken, S.; Gupta, H.; Gottlieb, C.A.; McCarthy, M.C.; Thaddeus, P. Detection of the Carbon Chain Negative Ion C8H-in TMC-1. *Astrophys. J.* **2007**, *664*, L43–L46. [CrossRef]

42. Cernicharo, J.; Guélin, M.; Agúndez, M.; Kawaguchi, K.; McCarthy, M.; Thaddeus, P. Astronomical Detection of C_4H^-, the Second Interstellar Anion. *Astron. Astrophys.* **2007**, *467*, L37–L40. [CrossRef]

43. Thaddeus, P.; Gottlieb, C.A.; Gupta, H.; Brünken, S.; McCarthy, M.C.; Agúndez, M.; Guélin, M.; Cernicharo, J. Laboratory and Astronomical Detection of the Negative Molecular Ion C_3N^-. *Astrophys. J.* **2008**, *677*, 1132–1139. [CrossRef]

44. Cernicharo, J.; Guélin, M.; Agúndez, M.; McCarthy, M.C.; Thaddeus, P. Detection of C_5N^- and Vibrationally Excited C_6H in IRC +10216. *Astrophys. J.* **2008**, *688*, L83–L86. [CrossRef]

45. Agúndez, M.; Cernicharo, J.; Guélin, M.; Kahane, C.; Roueff, E.; Klos, J.; Aoiz, F.J.; Lique, F.; Marcelino, N.; Goicoechea, J.R.; et al. Astronomical Identification of CN^-, the Smallest Observed Molecular Anion. *Astron. Astrophys.* **2010**, *517*, L2. [CrossRef]

46. Cami, J.; Bernard-Salas, J.; Peeters, E.; Malek, S.E. Detection of C_{60} and C_{70} in Young Planetary Nebulea. *Science* **2010**, *329*, 1180–1192. [CrossRef]

47. McGuire, B.A.; Burkhardt, A.M.; Kalenskii, S.; Shingledecker, C.; Remijan, A.J.; Herbst, E.; McCarthy, M.C. Detection of the Aromatic Molecule Benzonitrile (c-C_6H_5CN) in the Interstellar Medium. *Science* **2018**, *359*, 202–205. [CrossRef] [PubMed]

48. Hanel, R.; Conrath, B.; Flasar, F.M.; Kunde, V.; Maguire, W.; Pearl, J.; Pirraglia, J.; Samuelson, R.; Herath, L.; Allison, M.; et al. Infrared Observations of the Saturnian System from Voyager 1. *Science* **1981**, *212*, 192–200. [CrossRef]

49. López-Puertas, M.; Dinelli, B.M.; Adriani, A.; Funke, B.; García-Comas, M.; Moriconi, M.L.; D'Aversa, E.; Boersma, C.; Allamandola, L.J. Large Abundances of Polycyclic Aromatic Hydrocarbons in Titan's Upper Atmosphere. *Astrophys. J.* **2013**, *770*, 132. [CrossRef]

50. Molina-Cuberos, G.J.; Schwingenschuh, K.; López-Moreno, J.J.; Rodrigo, R.; Lara, L.M.; Anicich, V. Nitriles Produced by ion Chemistry in the Lower Ionosphere of Titan. *J. Geophys. Res. Planets* **2002**, *107*, 9–1–9–11. [CrossRef]

51. Kunde, V.; Aikin, A.C.; Hanel, R.A.; Jennings, D.E.; Maguire, W.; Samuelson, R.E. C_4H_2, HC_3N and C_2N_2 in Titan's Atmosphere. *Nature* **1981**, *292*, 686–688. [CrossRef]

52. Samuelson, R.; Hanel, R.; Kunde, V.; Maguire, W. Mean Molecular Weight and Hydrogen Abundance of Titan's Atmosphere. *Nature* **1981**, *292*, 688–693. [CrossRef]

53. Maguire, W.; Hanel, R.; Jennings, D.; Samuelson, V.K.R. C_3H_8 and C_3H_4 in Titan's Atmosphere. *Nature* **1981**, *292*, 683–686. [CrossRef]

54. Yung, Y.L.; Allen, M.; Pinto, J.P. Photochemistry of the Atmosphere of Titan-Comparison between Model and Observation. *Astrophys. Suppl. Ser.* **1984**, *55*, 465–506. [CrossRef]

55. Coates, A.J.; Crary, F.J.; Lewis, G.R.; Young, D.T.; Waite, J.H., Jr.; Sittler, E.C., Jr. Discovery of Heavy Negative Ions in Titan's Ionosphere. *Geophys. Res. Lett.* **2007**, *34*, L22103. [CrossRef]

56. Yung, Y. An Update of Nitrile Photochemistry on Titan. *Icarus* **1987**, *72*, 468–472. [CrossRef]

57. Bradforth, S.E.; Kim, E.H.; Arnold, D.W.; Neumark, D.M. Photoelectron Spectroscopy of CN^-, NCO^-, and NCS^-. *J. Chem. Phys.* **1993**, *98*, 800–810. [CrossRef]

58. Clifford, E.P.; Wenthold, P.G.; Lineberger, W.C.; Petersson, G.A.; Ellison, G.B. Photoelectron Spectroscopy of the NCN^- and $HNCN^-$ Ions. *J. Phys. Chem. A* **1997**, *101*, 4338–4345. [CrossRef]

59. Aoki, K.; Ikuta, S.; Murakami, A. Equilibrium Geometries and Stabilities of the C_3H Radical: Ab Initio MO Study. *J. Mol. Struct.* **1996**, *365*, 103–110. [CrossRef]

60. Moustefaoui, T.; Rebrion-Rowe, C.; Le Garrec, J.-L.; Rowe, C.-B.R.; Mitchell, J.B.A. Low Temperature Electron Attachment to Polycyclic Aromatic Hydrocarbons. *Faraday Discuss.* **1998**, *109*, 71–82. [CrossRef]

61. Dryza, V.; Sanelli, J.; Robertson, E.; Bieske, E. Electronic Spectra of Gas-Phase Polycyclic Aromatic Nitrogen Heterocycle Cations: isoquinoline+ and quinoline+. *J. Phys. Chem. A* **2012**, *17*, 4323–4329. [CrossRef]

62. Fortenberry, R.C.; Crawford, T.D. Singlet Excited States of Silicon-Containing Anions Relevant to Interstellar Chemistry. *J. Phys. Chem. A* **2011**, *28*, 8119–8124. [CrossRef] [PubMed]

63. Theis, M.L.; Candian, A.; Tielens, A.G.G.M.; Leec, T.J.; Fortenberry, R.C. Electronically Excited States of PANH anions. *Phys. Chem. Chem. Phys.* **2015**, *17*, 14761. [CrossRef] [PubMed]

64. Bassett, M.K.; Fortenberry, R.C. Symmetry Breaking and Spectral Considerations of the Surprisingly Floppy c-C_3H Radical and the Related Dipole-Bound Excited State of c-C_3H^-. *J. Chem. Phys.* **2017**, *146*, 224303. [CrossRef] [PubMed]

65. Theis, M.L.; Candian, A.; Tielens, A. G. G.M.; Lee, T.J.; Fortenberry, R.C. Electronically Excited States of Anisotropically Extended Singly-Deprotonated PAH Anions. *J. Phys. Chem. A* **2015**, *119*, 13048–13054. [CrossRef] [PubMed]

66. Fortenberry, R.C.; Moore, M.M.; Lee, T.J. Excited State Trends in Bidirectionally Expanded Closed-Shell PAH and PANH Anions. *J. Phys. Chem. A* **2016**, *120*, 7327–7334. [CrossRef] [PubMed]

67. Santaloci, T.J.; Fortenberry, R.C. On the Possibilities of Electronically Excited States in Stable Amine Anions: Dicyanoamine, Cyanoethynylamine, and diethynylamine. *Mol. Astrophys.* **2020**, *19*, 100070. [CrossRef]

68. Becke, A.D. Density-Functional Themochemistry. III. The Excact Exchange. *J. Chem. Phys.* **1993**, *98*, 5648. [CrossRef]

69. Frisch, M.J.; Trucks, G.W.; Schlegel, H.B.; Scuseria, G.E.; Robb, M.A.; Cheeseman, J.R.; Scalmani, G.; Barone, V.; Petersson, G.A.; Nakatsuji, H. *Gaussian~16 Revision C.01. 2016*; Gaussian Inc.: Wallingford, CT, USA, 2016.

70. Møller, C.; Plesset, M.S. Note on an Approximation Treatment for Many-Electron Systems. *Phys. Rev. J.* **1934**, *46*, 618–622. [CrossRef]

71. Chai, J.-D.; Head-Gordon, M. Long-Ranged Corrected Hybrid Density Functionals with Damped Atom-Atom Dispersion Corrections. *Phys. Chem. Chem. Phys.* **2008**, *10*, 6615–6620. [CrossRef]

72. Quynh, N.; Peters, W.; Fortenberry, R. Highly excited State Properties of Cumulenone Chlorides in the Vacuum-Ultraviolet. *Phys. Chem. Chem. Phys.* **2020**, *22*, 11838–11849.

73. Stanton, J.F.; Gauss, J.; Cheng, L.; Harding, M.E.; Matthews, D.A.; Szalay, P.G. CFOUR, Coupled-Cluster Techniques for Computational Chemistry, a Quantum-Chemical Program Package. Available online: http://www.cfour.de (accessed on 3 November 2019).

74. Werner, H.-J.; Knowles, P.J.; Knizia, G.; Manby, F.R.; Schütz, M. *MOLPRO, Version 2015.1, a Package of ab Initio Programs*; TTI— Technologie-Transfer-Initiative GmbH an der Universität Stuttgart (TTI GmbH): Stuttgart, Germany, 2015. Available online: http://www.molpro.net (accessed on 22 February 2012).

75. Krylov, A.I. Equation-of-Motion Coupled-Cluster Methods for Open-Shell and Electronically Excited Species: The Hitchhiker's Guide to Fock Space. *Annu. Rev. Phys. Chem.* **2008**, *59*, 433–462. [CrossRef] [PubMed]

76. Shavitt, I.; Bartlett, R. *MBPT and Coupled-Cluster Theory*; Many-Body Methods in Chemistry and Physics; Cambridge University Press: Cambridge, UK, 2009; Volume 59.

77. Stanton, R.; Bartlett, J.F. The Equation of Motion Coupled-Cluster Method—A Systematic Biorthogonal Approach to Molecular Excitation Energies, Transition-Probabilities, and Excited-State Properties. *J. Chem. Phys.* **1993**, *98*, 7029–7039. [CrossRef]

78. Kendall, R.A.; Dunning, T.H.; Harrison, R.J. Electron Affinities of the First-Row Atoms Revisited. Systematic Basis Sets and Wave Functions. *J. Chem. Phys.* **1992**, *96*, 6796–6806. [CrossRef]

79. Morgan, W.J.; Fortenberry, R.C. Additional Diffuse Functions in Basis Sets for Dipole-Bound Excited States of Anions. *Theor. Chem. Acc.* **2015**, *134*. [CrossRef]

80. Gulani, S.; Jahau, T.-C.; Sanov, A.; Krylov, A.I. The Quest to Uncover the Nature of Benzonitrile Anion. *Phys. Chem. Chem. Phys.* **2020**, *22*, 5002–5010. [CrossRef] [PubMed]

81. Stanton, J.F.; Gauss, J. Analytic Energy Derivatives for Ionized States Described by the Equation-of-Motion Coupled Cluster Method. *J. Phys. Chem.* **1994**, *101*, 8938–8944. [CrossRef]

82. Dunning, T.H. Gaussian Basis Sets for Use in Correlated Molecular Calculations. I. The Atoms Boron Through Neon and Hydrogen. *J. Chem. Phys.* **1989**, *90*, 1007–1023. [CrossRef]

83. Jenniskens, P.F. Desert A Survey of Diffuse Interstellar Bands (3800–8680 Å). *Astron. Astrophys. Suppl. Ser.* **1994**, *106*, 39–78.

84. Nichols, C.M.; Wang, Z.-C.; Yang, Z.; Lineberger, W.C.; Bierbaum, V.M. Experimental and Theoretical Studies of the Reactivity and Thermochemistry of Dicyanamide: $N(CN)_2^-$. *J. Phys. Chem. A* **2016**, *120*, 992–999. [CrossRef] [PubMed]

85. Dubois, D.; Sciamma-O'Brien, E.; Fortenberry, R.C. The Fundamental Vibrational Frequencies and Spectroscopic Constants of the Dicyanoamine Anion, $NCNCN^-$ ($C_2N_3^-$): Quantum Chemical Analysis for Astrophysical and Planetary Environments. *J. Astrophys.* **2019**, *883*, 109. [CrossRef]